

The Relativistic Binary Pulsar B1913+16

Joel M. Weisberg

*Department of Physics and Astronomy, Carleton College, Northfield,
MN, 55057 USA*

Joseph H. Taylor

Department of Physics, Princeton University, Princeton, NJ 08544 USA

Abstract. We describe the results of a relativistic analysis of our observations of binary pulsar B1913+16, up to the latest measurements in 2001 August.

1. Introduction

The relativistic binary pulsar B1913+16, discovered by Hulse & Taylor (1975), has now been observed for twenty-seven years. After a several-year hiatus due to the Arecibo upgrading project, we have resumed regular timing and profile measurements. In this paper, we describe the results of our relativistic analysis of these data.

2. Timing and Physical Parameter Extraction

In order to optimize timing data acquisition, we and colleagues have developed a number of specialized backends for recording binary and millisecond pulsar data, including a sweeping local oscillator system at 430 MHz (McCulloch, Taylor, & Weisberg 1979) and a succession of wideband samplers and signal averagers for use at 21 cm (Taylor & Weisberg 1982; Rawley 1986; Stinebring et al 1992). Most of our highest quality timing data were acquired with the Princeton Mark III backend (Stinebring et al 1992), which typically achieved time of arrival uncertainties $\Delta\text{TOA} \sim 16 \mu\text{s}$ in five-minute integrations of 40 MHz total bandwidth.

We have found that the quality of data acquired starting in 1981 are so much higher than earlier data that the previous measurements contribute negligibly to our fits. Consequently, we use 5083 TOAs measured between 1981 and 2001 in what follows. These TOAs were fed into program TEMPO (Taylor & Weisberg 1989; <http://pulsar.princeton.edu/tempo/>) which fitted for 18 parameters according to the phenomenological relativistic timing model of Damour & Deruelle (1985, 1986).

Aside from pulsar spin and astrometric parameters, we fitted for five “Keplerian” parameters and three relativistic quantities: projected semimajor axis of the pulsar orbit $a_p \sin i$, eccentricity e , reference epoch T_0 , binary orbital pe-

riod P_b , argument of periastron ω_0 , mean advance of periastron rate $\langle \dot{\omega} \rangle$, time dilation / gravitational redshift amplitude γ , and orbital period change rate \dot{P}_b .

Table 1. Measured Orbital Parameters

Fitted Parameter	Value	Uncertainty
$a_p \sin i$ (s)	2.341774	0.000001
e	0.6171338	0.0000004
T_0 (MJD)	46443.99588317	0.00000003
P_b (d)	0.322997462727	0.0000000000005
ω_0 (deg)	226.57518	0.00004
$\langle \dot{\omega} \rangle$ (deg/yr)	4.226607	0.000007
γ (s)	0.004294	0.000001
\dot{P}_b (10^{-12} s/s)	-2.4211	0.0014

The results for these eight fitted parameters, and their formal 1- σ uncertainties, are listed in Table 1. Only seven are required in order to specify completely all the orbital parameters and component masses except for an unknown rotation about the line of sight. For example the relativistic measurables $\langle \dot{\omega} \rangle$ and γ depend on the Keplerian parameters and the companion masses m_p and m_c in the following fashion:

$$\langle \dot{\omega} \rangle = 3 G^{2/3} c^{-2} (P_b/2\pi)^{-5/3} (1 - e^2)^{-1} (m_p + m_c)^{2/3}, \quad (1)$$

and

$$\gamma = G^{2/3} c^{-2} e (P_b/2\pi)^{1/3} m_c (m_p + 2m_c) (m_p + m_c)^{-4/3}. \quad (2)$$

Consequently measurement of the Keplerian parameters and $\langle \dot{\omega} \rangle$ and γ permits us to solve these two equations simultaneously for component masses, yielding $m_p = 1.4408 \pm 0.0003 M_\odot$; $m_c = 1.3873 \pm 0.0003 M_\odot$, where the uncertainty in the Newtonian Gravitational Constant G is not included. A graphical solution for the masses, also using Equations (1) and (2) and the same measurables, is shown in Figure 1.

These seven measured quantities and the parameters derived from them, such as m_p and m_c , are then adequate to derive all other interesting orbital parameters, such as the sine of the orbital inclination $\sin i$ and the various semimajor axes a , a_p , and a_c :

$$\sin i = G^{-1/3} c (a_p \sin i / m_c) (P_b/2\pi)^{-2/3} (m_p + m_c)^{2/3}, \quad (3)$$

$$a = G^{1/3} c^{-1} (P_b/2\pi)^{2/3} (m_p + m_c)^{1/3}, \quad (4)$$

$$a_p = a m_c (m_p + m_c)^{-1}, \quad (5)$$

and

$$a_c = a m_p (m_p + m_c)^{-1}. \quad (6)$$

In earlier datasets we also solved for the two parameters of the Shapiro gravitational delay, r and s , and we were marginally able to constrain them (Taylor and Weisberg 1989; Taylor et al 1992). As the orbit has precessed, however, the geometry has become less favorable for measuring this phenomenon. Continuing orbital precession is now causing the signature to begin to grow again.

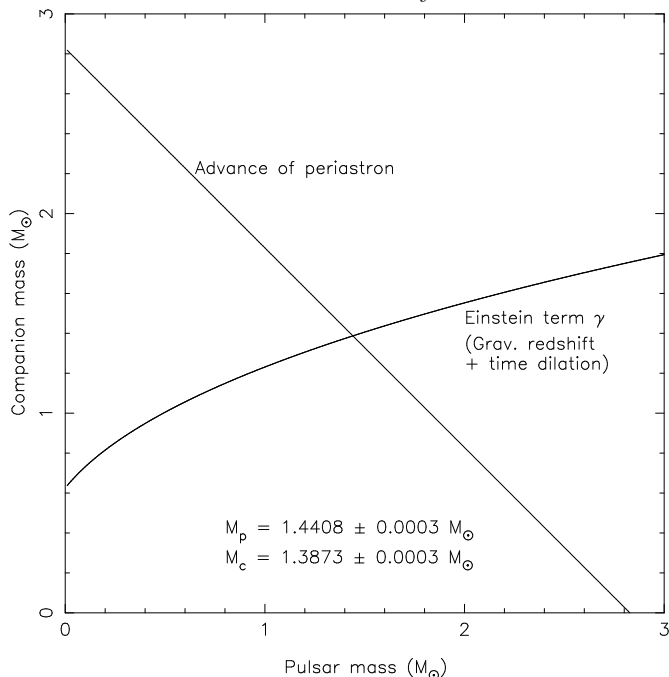


Figure 1. Constraints on the pulsar and companion mass from measurements of the “Keplerian” orbital elements plus relativistic advance of periastron $\langle\dot{\omega}\rangle$ and the “Einstein” term γ . The uncertainties in $\langle\dot{\omega}\rangle$ and γ are smaller than the displayed linewidths.

3. Gravitational Radiation Emission

The emission of gravitational radiation should lead to orbital energy loss and orbital decay. This will be observable as an orbital period change, \dot{P}_b . According to general relativity, the orbital period change due to gravitational radiation damping will depend on the system parameters as follows:

$$\dot{P}_b = -\frac{192 \pi G^{5/3}}{5 c^5} \left(\frac{P_b}{2\pi}\right)^{-5/3} (1 - e^2)^{-7/2} \times \left(1 + \frac{73}{24}e^2 + \frac{37}{96}e^4\right) m_p m_c (m_p + m_c)^{-1/3}. \quad (7)$$

Inserting our measured values of the parameters given in Table 1 into Equation (7), we calculate that the general relativistic prediction for orbital period decay rate is $\dot{P}_b_{GR} = (-2.40247 \pm 0.00002) \times 10^{-12}$ s/s.

The galactic acceleration of the system and the Sun also cause an orbital period change, $\dot{P}_{b,gal}$ (Damour & Taylor 1991). Using their Equation (2.12) and their parameters for $(\dot{P}_b/P_b)_{gal}$ [except for the following updated parameters: solar galactocentric distance $R_0 = 8.0 \pm 0.5$ kpc (Reid 1993); pulsar distance $d = 5.90 \pm 0.94$ kpc (Cordes & Lazio 2002); solar galactocentric circular velocity $v_0 = 224 \pm 16$ km / s (Reid et al 1999, Backer & Sramek 1999); pulsar proper motion $\mu = 2.6 \pm 0.3$ mas / yr], we find that $\dot{P}_{b,gal} = -(0.0125 \pm 0.0050) \times 10^{-12}$ s/s. The galactic quantities will be improved in the next several years with

additional interferometric observations of Sgr A* and infrared measurements of stars orbiting it (Salim & Gould 1999; Ghez et al 2000; Schodel et al 2002).

Correcting the observed orbital period derivative for the galactic acceleration term,

$$\dot{P}_b \text{ corrected} = \dot{P}_b \text{ observed} - \dot{P}_b \text{ gal}, \quad (8)$$

we find $\dot{P}_b \text{ corrected} = -(2.4086 \pm 0.0052) \times 10^{-12}$ s/s, in good agreement with the theoretical general relativistic result $\dot{P}_b \text{ GR}$ given above. The comparison is also shown graphically in Figure 2, where we plot the observed and general relativistically predicted shift of periastron time resulting from gravitational radiation damping.

This result provides strong confirmation of the existence of gravitational radiation as predicted by general relativity. Weisberg & Taylor (1981) show that it rules out numerous other relativistic theories of gravitation. This result plus relativistic measurements of other binary pulsars also constrain the parameters of viable tensor–scalar theories (Taylor et al 1992; Damour & Esposito-Farese 2001).

4. Geodetic Spin Precession

The spinning, orbiting pulsar should also experience geodetic precession, which is caused by general relativistic gravitomagnetic spin–orbit coupling (Damour & Ruffini 1974; Barker & O’Connell 1975a,b). This will lead to a change in the observed pulseshape as the Earth–pulsar line of sight cuts across different parts of the precessing beam. Weisberg, Romani, & Taylor (1989) noted the first pulseshape changes ascribed to geodetic precession. The pattern became clearer when Kramer (1998) detected a secular narrowing of the separation between the two principal pulse components, which he was able to successfully model. Weisberg & Taylor (2002) measured shape changes throughout the pulse in twenty years of Arecibo 21 cm data. The pulse profile was divided into even and odd components to separate overall beam structure from patchy structure, respectively. We found that the outer skirts of the even profile barely changed while the peaks drew closer and the central saddle filled in (Figure 3a). Our model that best fits these data indicates an hourglass-shaped beam elongated in the latitude direction (Figure 3b). Interestingly, Link & Epstein (2001) found a similar beam shape for a (nonrelativistically) precessing pulsar, B1828-11. See also Kramer (this volume) for additional observations and modeling.

Acknowledgments. We thank the National Science Foundation for supporting this project since its inception (most recently through grants AST 00-98540 and 96-18357), and the staff of Arecibo Observatory for their enthusiastic help. Arecibo Observatory is operated by Cornell University under cooperative agreement with the NSF.

References

Backer, D. C. & Sramek, R. A. 1999, *ApJ*, 524, 805

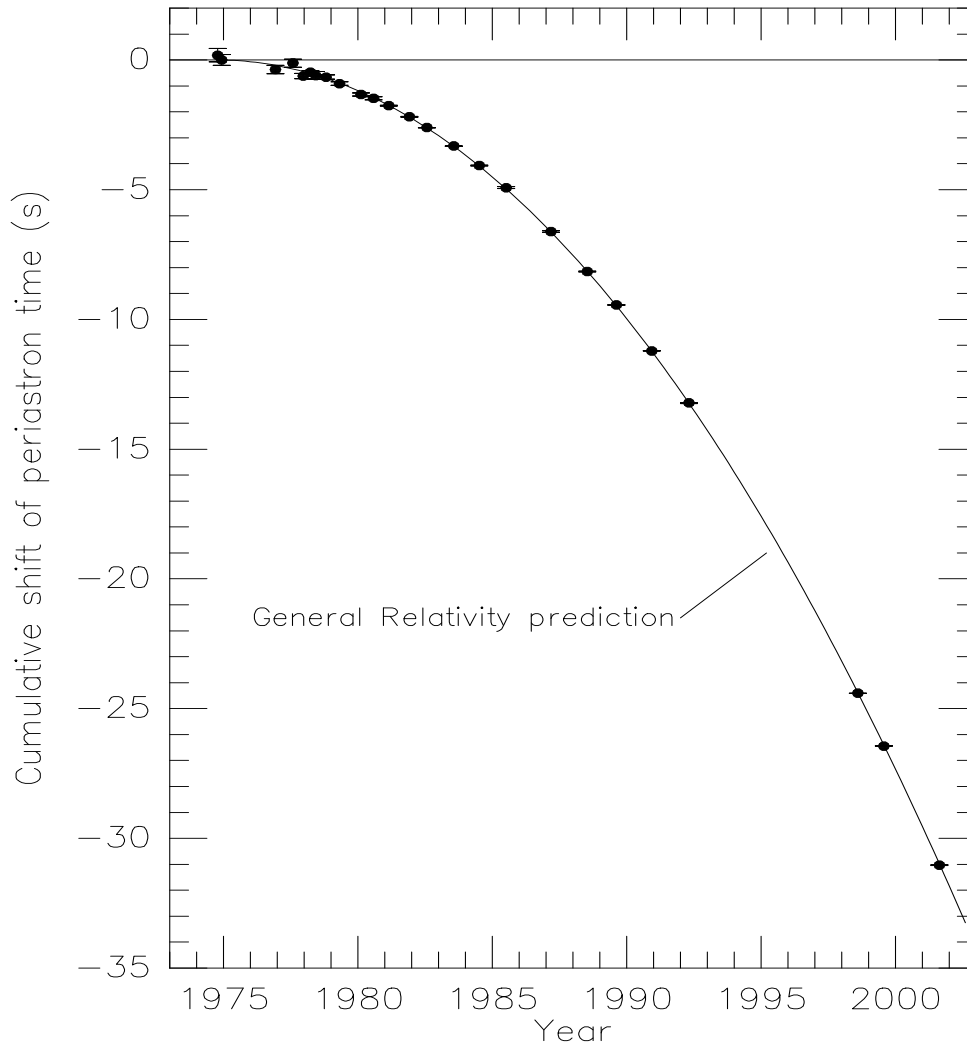


Figure 2. Gravitational radiation damping should cause orbital decay which leads to an accumulating shift in epoch of periastron. The parabola illustrates the general relativistically predicted shift, while the observations are marked by data points. In most cases (particularly in the later data), the measurement uncertainties are smaller than the line widths.

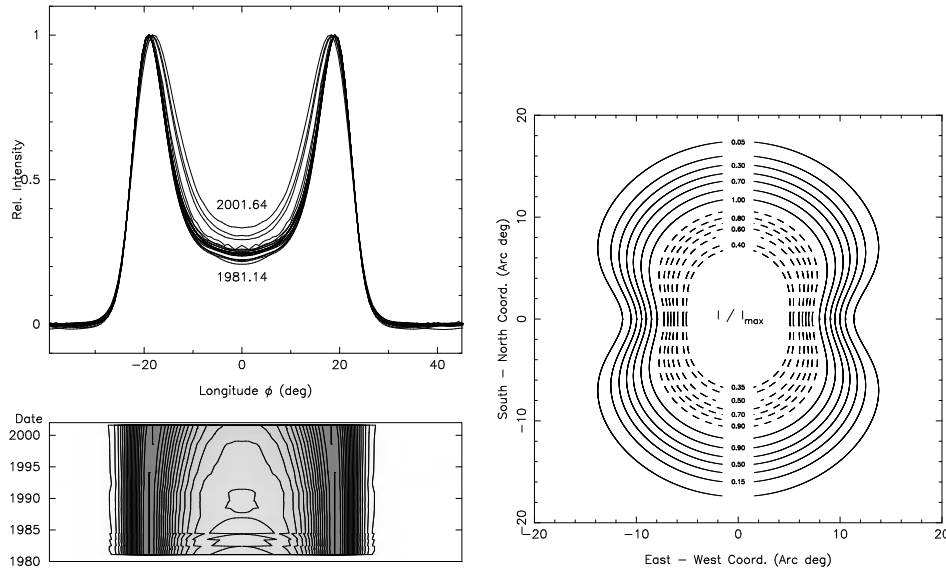


Figure 3. Left: Even component of B1913+16 pulse profile at 21 cm versus date. Right: Our inferred best-fitting emission beam model.

- Barker, B. M. & O'Connell, R. F. 1975a, *Phys.Rev.D*, 12, 329
 Barker, B. M. & Oconnell, R. F. 1975b, *ApJ*, 199, L25
 Cordes, J. M. & Lazio, T. J. W. 2002, astro-ph 0207156
 Damour, T. & Ruffini, R. 1974, *Academie des Sciences Paris Comptes Rendus Serie Sciences Mathematiques*, 279, 971
 Damour, T. & Deruelle, N. 1985, *Ann. Inst. H. Poincare (Phys. Theorique)*, 43, 107
 Damour, T. & Deruelle, N. 1986, *Ann. Inst. H. Poincare (Phys. Theorique)*, 44, 263
 Damour, T. & Taylor, J. H. 1991, *ApJ*, 366, 501
 Damour, T. & Esposito-Farese, G. 2001, *Phys.Rev.D*, 58, 042001
 Ghez, A. M., Morris, M., Becklin, E. E., Tanner, A., & Kremenek, T. 2000, *Nature*, 407, 349
 Hulse, R. A. & Taylor, J. H. 1975, *ApJ*, 195, L51
 Kramer, M. 1998, *ApJ*, 509, 856
 Link, B. & Epstein, R. I. 2001, *ApJ*, 556, 392
 McCulloch, P. M., Taylor, J. H., & Weisberg, J. M. 1979, *ApJ*, 227, L133
 Rawley, L. A. 1986, Ph. D. thesis, Princeton U.
 Reid, M. J. 1993, *ARA&A*, 31, 345
 Reid, M. J., Readhead, A. C. S., Vermeulen, R. C., & Treuhaft, R. N. 1999, *ApJ*, 524, 816
 Salim, S. & Gould, A. 1999, *ApJ*, 523, 633
 Schodel, R., et al 2002, *Nature*, 694

- Stinebring, D. R., Kaspi, V. M., Nice, D. J., Ryba, M. F., Taylor, J. H., Thorsett, S. E., & Hankins, T. H. 1992, *Review of Scientific Instruments*, 63, 3551
- Taylor, J. H. & Weisberg, J. M. 1982, *ApJ*, 253, 908
- Taylor, J. H., & Weisberg, J. M. 1989, *ApJ*, 345, 434
- Taylor, J. H., Wolszczan, A., Damour, T., & Weisberg, J. M. 1992, *Nature*, 355, 132
- Weisberg, J. M. & Taylor, J. H. 1981, *Gen. Rel. & Grav.*, 13, 1
- Weisberg, J. M., Romani, R. W. , & Taylor, J. H. 1989, *ApJ*, 347, 1030
- Weisberg, J. M. & Taylor, J. H. 2002, *ApJ*, 576, 942